Master in Aerospace Engineering

Research project semester 3 report

Low Thrust Homotopy: GPOPS-II approach

Supervisors:
Joan-Pau Sanchez Cuartielles
Jose-Carlos Garcia Mateas

Author:
Andrea Ruscica

March 24, 2025

Declaration of Authenticity

This assignment is entirely my own work. Quotations from literature are properly indicated with appropriated references in the text. All literature used in this piece of work is indicated in the bibliography placed at the end. I confirm that no sources have been used other than those stated.

I understand that plagiarism (copy without mentioning the reference) is a serious examinations offence that may result in disciplinary action being taken.

Contents

List of Figures

1 Abstract

Low-thrust propulsion systems, typically in the form of electric propulsion, offer remarkable advantages for economical space access. Their high specific impulse, generally an order of magnitude greater than conventional chemical engines, enables substantial reduction of onboard propellant requirements for missions, maximizing payload capacity or reducing launch costs. However, the inherent low-thrust characteristics of these systems present significant challenges for mission designers, as the thrust cannot be modeled as instantaneous, complicating both mission design and optimization processes. This work investigates the application of DMG, a modified version of the general-purpose optimizer GPOPS-II, to complex multi-body low-thrust transfers in the context of the GTOC-4 challenge. Different state representations (Cartesian State Vectors and Modified Equinoctial Elements), optimization strategies, and initial guess approaches were analyzed and compared. Results demonstrate that sequential optimization of trajectory segments is computationally more efficient than whole-trajectory optimization while maintaining solution quality. The study successfully verified the feasibility of the Johnson solution under GTOC-4 constraints, achieving a final spacecraft mass of 550.95 kg with all thrust values below the 0.135 N limit. The analysis highlights the critical importance of high-quality initial guesses and appropriate scaling procedures for ensuring convergence in these numerically challenging problems.

Keywords: Low Thrust, GPOPS-II, DMG, GTOC.

2 Introduction

Low-thrust propulsion systems represent a significant advancement in spacecraft propulsion technology, offering substantial benefits in terms of fuel efficiency. Unlike traditional chemical propulsion systems that provide high thrust for short periods of time, low-thrust systems generate modest acceleration over extended periods with much higher specific impulse, which makes them suitable for long-duration missions, including deep space exploration and asteroid rendez-vous.

The optimization of low-thrust trajectories presents numerous complex challenges that distinguish it from high-thrust trajectory planning. The continuous nature of low-thrust propulsion requires trajectory optimization over extended time periods. While high-thrust missions can often be modeled as a series of discrete impulses separated by coast arcs, low-thrust missions involve continuous control throughout the trajectory, significantly increasing the dimensionality of the optimization problem. Furthermore, low-thrust trajectory optimization typically involves highly nonlinear dynamics and constraints. The coupling between the spacecraft state and control variables creates a complex solution space characterized by a number of local optima, making it difficult to identify globally optimal solutions. The extended mission durations associated with low-thrust propulsion introduce sensitivity to perturbations and model uncertainties. Small errors in modeling or execution can accumulate over time, potentially rendering solutions infeasible or suboptimal.

The use of DMG, a modified and open source version of GPOPS-II, was investigated in the context of the solutions proposed for the GTOC-4 challenge.

2.1 The GTOC-4 challenge

The *Global Trajectory Optimization Challenge* is an international challenge organised by ESA [1] to solve complex trajectory design problems. In particular, the fourth edition of the challenge, hosted in 2009, had as its main goal visiting as many Near Earth Asteroids (NEAs) as possible within 10 years of the spacecraft launch. NEAs are classified as asteroids whose perihelion is less than 1.3 AUs. The winning team from the Moscow State University managed to visit 44 asteroids with a final mass of 553.46 kg. Another paper has been published [3] in which the team claims to have found a solution to visit 49 asteroids. Investigating the feasibility of this solution via the use of the DMG toolbox will be the main scope of this report. In Table 1 the spacecrafts data are presented.

Parameter	**Value**	**Unit**
Initial mass	1500	kg
Maximum thrust	0.135	N
Specific impulse	3000	s
Minimum final mass	500	kg
Maximum mission duration	10	years

Table 1: Spacecraft and Mission Parameters for GTOC-4

3 Problem Dynamics

As the spacecraft is supposed to fly in outer space, it is reasonable to assume that the only forces acting on it are the Sun gravitational pull and the thrust of the engine. The system can therefore be modelled as a perturbed two body problem (P2BP). Given the parameters in Table 1, the thrust acceleration is in the order of 10^{-5} m/s^2 and therefore can be considered as a perturbation with respect to the gravitational pull, which is in the order of 10^{-3} m/s^2. The state of the system and its dynamics can be expressed in multiple reference frames. In the context of this work, Cartesian State Vector (CVS) and Modified Equinoctial Elements (MEE) have been used.

3.1 Cartesian State Vector (CSV)

In a cartesian reference system, the P2BP can be expressed as:

$$\ddot{\mathbf{r}} = -\mu \frac{\mathbf{r}}{r^3} + \mathbf{a} \tag{1}$$

$$\mathbf{a} = \frac{\mathbf{T}}{m} \tag{2}$$

Where $\mathbf{r}$ is the radius of the orbit of the spacecraft, $\mathbf{a}$ is the acceleration produced by the low thrust engine, m its mass and $\mathbf{T}$ is the thrust vector in such reference frame.

This vector equation can be projected into the x,y,z axis:

$$\begin{cases} \ddot{x} = -\mu \frac{x}{r^3} + a_x \\ \ddot{y} = -\mu \frac{y}{r^3} + a_y \\ \ddot{z} = -\mu \frac{z}{r^3} + a_z \end{cases} \tag{3}$$

Where $r = \sqrt{x^2 + y^2 + z^2}$ is the norm of the position vector. The acceleration resulting from the thrust in each of the axis can be expressed as follows:

$$\begin{cases} a_x = \frac{T}{m} \cdot \cos\alpha \cdot \cos\beta \\ a_y = \frac{T}{m} \cdot \sin\alpha \cdot \cos\beta \\ a_z = \frac{T}{m} \cdot \sin\beta \end{cases} \tag{4}$$

Where α and β are defined as in Figure 1 as something analogous to azimuth and elevation. The origin of the reference system is considered to be the Sun, and the (x,y,z) axis are defined as 3 perpendicular unitary vectors.

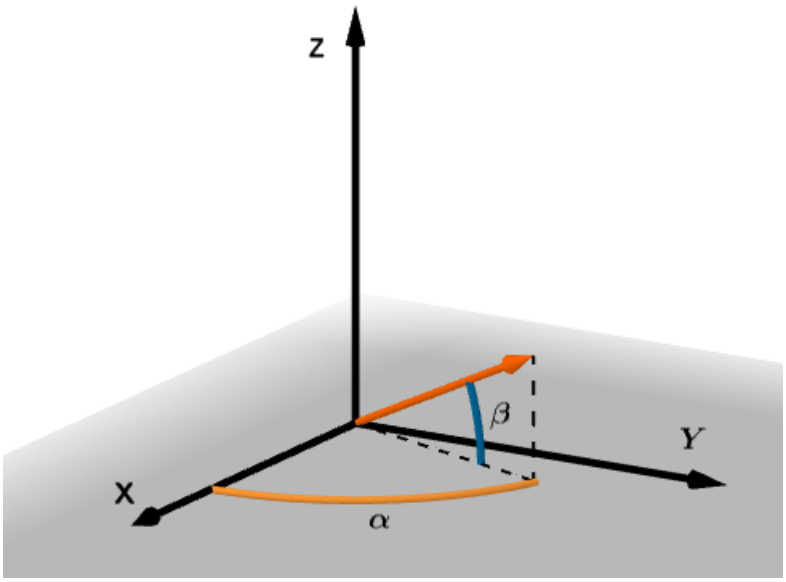

Figure 1: Angles definition in a CSV representation

3.2 Modified Equinoctial Elements (MEE)

Modified Equinoctial Elements are a set of orbital elements valid for circular, elliptic and hyperbolic orbits developed to address some of the problems and singularities of the classical orbital elements, as well as to be more suitable for numerical optimization than a CSV representation [7]. The set of 6 MEEs are:

$$\begin{cases} p = a(1-e^2) \\ f = e \cdot \cos(\omega + \Omega) \\ g = e \cdot \sin(\omega + \Omega) \\ h = \tan(i/2) \cdot \cos\Omega \\ k = \tan(i/2) \cdot \sin\Omega \\ L = \Omega + \omega + \theta \end{cases} \tag{5}$$

The dynamics of the system expressed via the MEE is as follow [7]:

$$\begin{cases} \dot{p} &= \frac{dp}{dt} = \frac{2p}{w}\sqrt{\frac{p}{\mu}}\Delta_t \\ \dot{f} &= \frac{df}{dt} = \sqrt{\frac{p}{\mu}}\left[\Delta_r \sin L + [(w+1)\cos L + f]\frac{\Delta_t}{w} - (h\sin L - k\cos L)\frac{g\Delta_n}{w}\right] \\ \dot{g} &= \frac{dg}{dt} = \sqrt{\frac{p}{\mu}}\left[-\Delta_r \cos L + [(w+1)\sin L + g]\frac{\Delta_t}{w} + (h\sin L - k\cos L)\frac{g\Delta_n}{w}\right] \\ \dot{h} &= \frac{dh}{dt} = \sqrt{\frac{p}{\mu}}\frac{s^2\Delta_n}{2w}\cos L \\ \dot{k} &= \frac{dk}{dt} = \sqrt{\frac{p}{\mu}}\frac{s^2\Delta_n}{2w}\sin L \\ \dot{L} &= \frac{dL}{dt} = \sqrt{\mu p}\left(\frac{w}{p}\right)^2 + \frac{1}{w}\sqrt{\frac{p}{\mu}}(h\sin L - k\cos L)\Delta_n \end{cases} \tag{6}$$

Where Δ_r, Δ_t and Δ_n are the perturbations accelerations in a RTN (Radial, Tangential, Normal) frame of reference.

The acceleration due to the thrust can be expressed as:

$$\mathbf{a_T} = \frac{T}{m}\hat{\mathbf{u}} \tag{7}$$

Where $\hat{\mathbf{u}} = [u_r, u_t, u_n]$ is the unit vector pointing in the direction of the thrust expressed in the same RTN frame. To convert a unit vector from a cartesian reference frame to RTN, relation 8 can be used:

$$\hat{\mathbf{u}}_{\mathbf{ECI}} = \left[\hat{\mathbf{i}}_{\mathbf{r}}, \quad \hat{\mathbf{i}}_{\mathbf{t}}, \quad \hat{\mathbf{i}}_{\mathbf{n}}\right] \cdot \hat{\mathbf{u}}_{\mathbf{MEE}} \tag{8}$$

in which:

$$\hat{\mathbf{i}}_{\mathbf{r}} = \frac{\mathbf{r}}{|\mathbf{r}|}, \qquad \hat{\mathbf{i}}_{\mathbf{n}} = \frac{\mathbf{r}\times\mathbf{v}}{|\mathbf{r}\times\mathbf{v}|}, \qquad \hat{\mathbf{i}}_{\mathbf{t}} = \hat{\mathbf{i}}_{\mathbf{n}} \times \hat{\mathbf{i}}_{\mathbf{r}} \tag{9}$$

4 State of the art

In literature, many methods and algorithms can be found on low-thrust trajectory optimization, applied to many of the most common scenarios, such as orbit raising or interplanetary transfers.

4.1 Analytical solutions

Analytical solutions can be found only for very simple cases and particular control profiles. As stated in [5], two easy to implement and widely used models for obtaining analytical solutions of low-thrust transfers are the Kepler and Stark Model.

- Kepler Model: This model simplifies the continuous evolution of the system with a series of instantaneous velocity impulses, connected by a coasting arc without any thrust applied.
- Stark Model: In this model, the thrust profile is simplyfied as series of accelerations constant in magnitude and direction. As such, it is a little bit more complex than the Kepler model.

Further analytical solutions can be found for very particular continuous thrust profile such as constant tangential or radial thrust. For more complex optimization problems, that allow for more complex thrust profiles, numerical procedures are essential as analytical solutions do not exist or are extremely difficult to find.

4.2 Numerical Methods

Numerical methods allow to tackle far more complex problems than what it is possible to achieve with exact, but limited analytical models. As stated in [5], there are 3 main methods to solve such numerical problems: *Indirect methods*, *Direct methods* and *Dynamic programming*. Indirect methods apply the Pontryagin's maximum principle, which is a first order necessary optimality condition. These methods are suitable to obtain a continuous control profile at each instant. Direct methods, on the other hand, convert the continuous problem into a Nonlinear Programming Problem (NLP) with a discretized time grid and try to find an optimal solution by applying the Karush-Kuhn-Tucker conditions (KKT). Both direct and indirect methods can implement one of the following techniques to impose the dynamical equations [5]: *Single shooting*, *multiple shooting* or *collocation*. Each of them differs in how they integrate and impose the boundary conditions and constraints on the solution. Lastly, Dynamical programming utilises *Bellman's principle of optimality*, which stems from the *Hamilton-Jacobi-Bellman* theorem.

Furthermore, both Direct and Indirect methods can be solved by gradient-based methods such as SNOPT, NPSOL and *IPOPT* or by a Heuristic search such as evolutionary algorithms.

4.3 The Sims-Flanagan Model

The Sims-Flanagan Model, presented in 1999 by Sims and Flanagan [6] is a direct method in which the trajectory of the spacecraft is divided into *legs* that start and finish at so-called *control nodes*. Each of the legs has a Match point where continuity conditions for the mass, position and velocity must be applied to obtain a feasible trajectory. The trajectory is then propagated forward in time from the leg initial control node to the match point and backwards in time from the final control node to the match point. every leg is then divided into *segments*, where the Low-Thrust action is modelled as impulsive ΔVs in the middle point of each segment. After each impulse, the trajectory is propagated as a keplerian orbit without any perturbation.

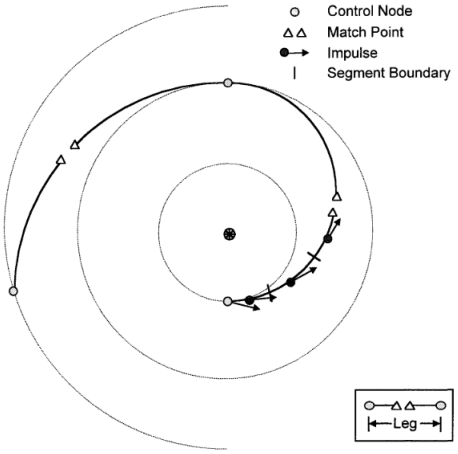

Figure 2: Sims-Flanagan model. From [6]

The trajectory obtained with this method can then be optimized by many algorithms to find the optimal solution with respect to a given optimization parameter. Moreover, this method can be use to generate initial guesses for other optimization algorithms.

4.4 GPOPS-II and DMG

GPOPS-II (General Purpose Optimal Control Software) is a general purpose optimizer that uses Gaussian quadrature collocation to solve optimal control problems. Low-Thrust trajectories can therefore be studied and optimized via the use of this software. It is distributed via a paying licence. David Morante Gonzalez developed a version of the toolbox [2], DMG, from an open-source version of GPOPS and he adapted it to work with the open-source IPOPT (Interior point optimizer) solver instead of the proprietary SNOPT. In addition, the *Hermite-Simpson* collocation scheme has been implemented into the toolbox to transcribe the optimal control problem into a NLP.

4.5 DMG

As previously stated, DMG is a modified version of GPOPS-II. A complete explanation of its syntax and parameters can be found in DMG's user manual [2]. A summary of the toolbox structure and parameters is hereby presented:

To build an optimal control problem in DMG, the following functions must be provided:

- **Cost functional:** the objective function that it is needed to minimize. It outputs the Mayer and Lagrange cost for each phase of the problem. The first is a scalar value that that represents the parameter to be optimized at the end of each phase. The latter is a vector that has to be minimized at each point during each phase.
- **The Differential-Algebraic Equations (DAEs):** the differential equations that govern the system, as well as the path constraints, which are constraints to be satisfied at every point of the trajectory.
- **Events constraints:** The boundary condition that must be satisfied at the beginning or end of each phase.
- **Linkage constraints:** They define which parameters must be continuous at the interface between each phase.

Bounds on the state (at the start, during and at the end of each phase), on the controls, on the static parameters (if any) and on the duration and the boundary conditions must be provided. A tolerance on the linkage between phases is also necessary.

Imposing a final condition can be done in 2 ways: Either through an event constraint or by setting the minimum and maximum bounds for the final state equal to the desired final state. The second method is fine when the problems consists in only one phase, but becomes more cumbersome coding-wise when two or more phases are considered.

Another crucial aspect for DMG is the choice of a suitable initial guess. For the solver to converge to an optimal solution (or even to converge at all), the initial guess must be sufficiently close to such a solution.

DMG has been modified to work with the NLP solver IPOPT (Interior Point Optimizer). This solver can use many methods. In this context, the *pseudospectral* method and the *Hermite-Simpson* method have been used. In addition, the scaling of the problem is an important thing to consider for numerical stability and for convergence. The pseudospectral methods has an autoscale feature that automatically scales the problem. The Hermite-Simpson method, on the other hand, does not have such feature, therefore it is important to manually scale the problem.

5 Semester 3

5.1 Semester 2 recalls and summary

In this section, a brief recall of the work done in semester 2 is presented. Most of the work consisted of setting up the optimization problem and evaluating which parameters were important to focus on. After an initial phase consisting in the validation of the DMG tool, The work focused exclusively on the study of the extended Moscow solution, in which the authors claim to have found a feasible trajectory visiting 49 asteroids.

Various initial guesses were considered for the analysis of such solution, such as simple keplerian propagation, a constant thrust in the direction of the next asteroid or the second next asteroid, and initial guesses created via the Sims-Flanagan model. Only the latter satisfies the constraint on the final position of each asteroids.

A scaling procedure was implemented only for the CSV representation. The following scaling values were used:

- lenght $l_c = 1$ AU;
- gravitational parameter $\mu = 1.327124 \cdot 10^{11}$ km^3/s^2
- mass $m_c = 1500$ kg

Every other quantities have been derived from those. The steering angle α and β were not scaled.

After a period of validation of the DMG toolbox, the work focused on trying to optimize single arcs of the Moscow solution, using as the initial state the position of the initial asteroid in the official solution, the velocity of the Lambert's arc from the previous asteroid to the initial asteroid and the initial mass of the official solution at the asteroid first fly by. The final state was imposed as an event constraint.

Three main objective functions were considered:

- Mayer = 0. This objective function does not optimize for any variables, but instead focuses on finding a solution that satisfies the constraint. It can be used as an initial guess for further refinement.
- Mayer = -w_f. The goal here is to maximize the weight at the end of the arc, thus minimizing propellant consumption.
- Mayer = $\delta_x^2 + \delta_y^2 + \delta_z^2$. Where δ is the difference between the end velocity of the arc after the optimization and the initial velocity of the next Lambert arc, decomposed on the 3 cartesian axis. The goal of this objective function was to try to steer the solution towards a final state that would be favorable for the convergence of the next arc. The Lambert arc represents the optimal impulsive transfer between 2 points with a given Time of flight. If the initial velocity of the arc is already the Lambert arc initial velocity, it means that no thrusting is necessary to arrive to the next arc. So, if the thrust necessary varies in a continuous manner, the smaller the velocity error is, the less thrusting is necessary during the arc.

Finally, multiple-phases problems were considered. The linkage at each phase interface was set to make the state (position, velocity and mass for CSV or MEEs and mass for MEE) continuous. To achieve this, it was imposed that:

$$S_{init}^{i+1} - S_{final}^{i} = 0.$$

Where S is the state at the ith phase. Thus, no tolerance was set on the linkage constraints.

Analyzing various arc, it was evident that minimizing δ^2 was not a good strategy, as the final velocity difference for most arc was higher than the one obtained simply by optimizing for the mass.

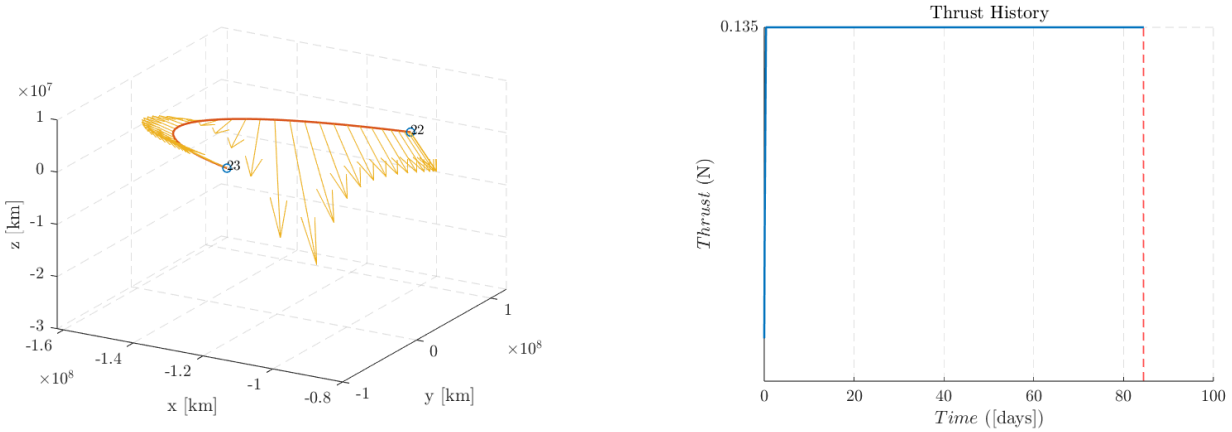

(a) Trajectory with Thrust vectors in arc 22.

(b) Thrust profile in arc 22.

Figure 3: Arc 22, optimizing $|\delta|^2$, solved to acceptable solution.

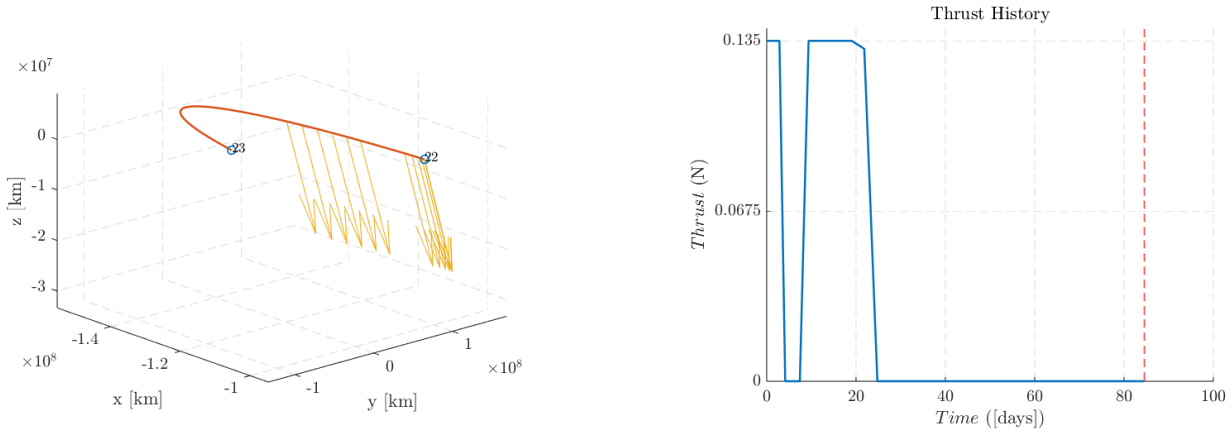

(a) Trajectory with Thrust vectors in arc 22.

(b) Thrust profile in arc 22.

Figure 4: Arc 22, optimizing the final weight, solved to acceptable solution.

In Figure 3 the trajectory and thrust profile for arc 22 of the Moscow solution is presented. Optimizing for δ^2, the difference between the final velocity and the next lambert arc velocity was $|\delta| = 0.5456$ km/s, while just optimizing for the mass a value of $|\delta| = 0.4262$ km/s was achieved, highlighting the poor performances of such objective function.

Multiple arc trajectory optimization proved successful when arcs were linked together, demonstrating better convergence characteristics than when attempted individually. Several arc combinations (3-8, 17-29, 22-29, and 43-45) successfully converged with a maximum thrust of 0.135 N, whereas other combinations failed to converge or required higher thrust levels. For example, arc combinations 0-2 and 22-30 did not converge with the GTOC4 thrust, requiring maximum thrust values of 0.17 N and 0.2 N respectively.

Two optimization approaches were compared: one focused only on meeting trajectory constraints without additional optimization, and the other aimed at minimizing the final spacecraft weight. The weight optimization approach resulted in more aggressive thrust profiles characterized by sharper engine switching patterns. This difference is clearly illustrated in the thrust history graphs for arcs 25-30, where the weight-optimized solution shows more defined thrust variations compared to the non-optimized approach.

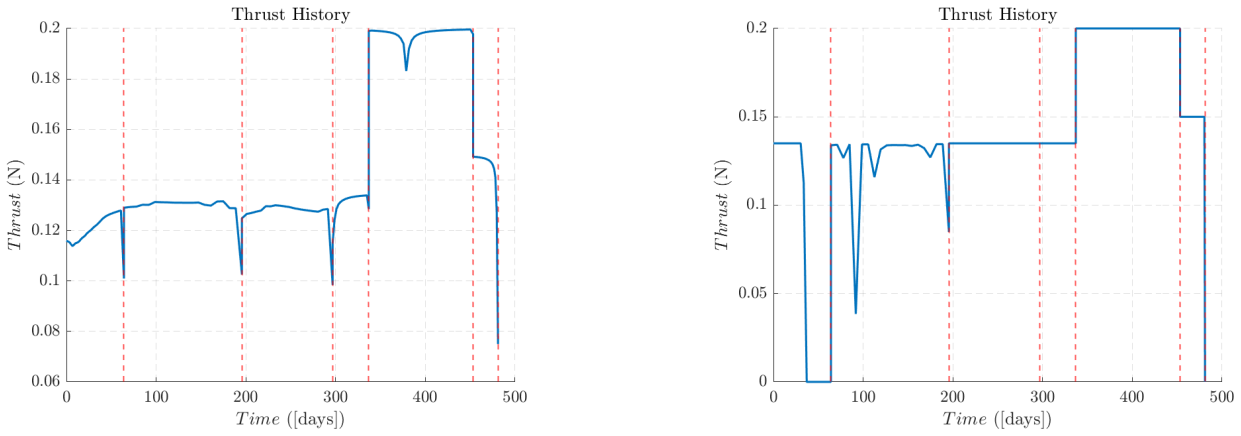

(a) Thrust History, no opt.

(b) Thrust History, maximizing weight.

Figure 5: Multiple arcs trial.

For problematic trajectory segments, it was found that initiating the optimization from arcs located three or more segments away provided the spacecraft sufficient time to correct its state before encountering challenging trajectory segments. This strategy proved effective in managing the "wrong" initial conditions that might otherwise prevent convergence.

The full Moscow solution was analyzed using a maximum thrust of 0.2 N for each trajectory leg. This comprehensive analysis yielded a final spacecraft mass of 501 kg, just barely respecting the 500 kg constraint, with an average thrust of 0.1014 N across the mission duration. The thrust and mass histories show a gradually decreasing mass profile and variable thrust requirements throughout the approximately 3500-day mission.

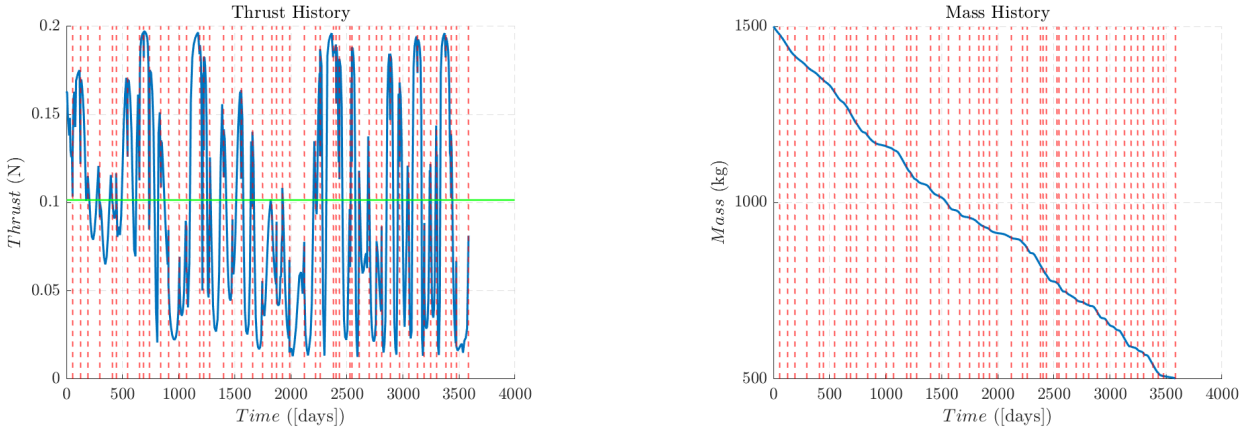

(a) Thrust History.

(b) Mass History.

Figure 6: Moscow solution.

Sequential optimization of trajectory sections proved computationally less expensive than attempting to optimize all arcs simultaneously. This approach involved optimizing trajectory segments incrementally, starting from the departure arc and proceeding sequentially. However, the analysis revealed that a maximum thrust of 0.135 N was insufficient for the second arc, indicating the need for higher thrust capabilities or alternative trajectory designs for this segment.

5.2 Semester 3 goal and objectives

This part of the report will tackle the work done during the third semester. The work continued to study the feasibility of low-thrust trajectories for the GTOC-4 challenge, being adapted to solutions different than the Moscow solution, which revealed itself to be quite challenging for the optimization. First, a scaling procedure for the modified equinotcial element (MEE) representation was implemented. After, the study of the *Johnson solution* of the GTOC-4 was conducted, utilizing the first guesses provided by the work on the Sims-Flanagan method and a sequential approach. It was possible to obtain a feasible solution for such trajectory with a final mass of 550.95 kg. The same approach was utilized for a modified version of the Moscow Solution, but to no avail.

6 Investigation Methods

This study employed a systematic approach to investigate low-thrust trajectory optimization using the DMG toolbox, a modified version of GPOPS-II that works with the open-source IPOPT solver.

Two primary state representations were evaluated throughout the investigation: Cartesian State Vectors (CSV) and Modified Equinoctial Elements (MEE). For each representation, appropriate scaling procedures were implemented to improve numerical stability. The CSV scaling used the reference quantities presented in subsection 5.1. For the MEE representation, a similar scaling approach is hereby presented.

6.1 Scaling procedure for MEEs

In this section, a scaling procedure for the modified equinoctial elements (MEE) representation is presented. As for the CSV case, this scaling procedure is supposed to make the numerical optimization problem easier for the optimizer by using smaller values and similar to each other. Using the same reference quantities as in

subsection 5.1, the MEE dynamics equations can be written as:

$$\begin{cases} \dot{p} &= \frac{dp}{dt} = \frac{2p}{w}\sqrt{p}\Delta_t \\ \dot{f} &= \frac{df}{dt} = \sqrt{p}\left[\Delta_r \sin L + [(w+1)\cos L + f]\,\frac{\Delta_t}{w} - (h\sin L - k\cos L)\frac{g\Delta_n}{w}\right] \\ \dot{g} &= \frac{dg}{dt} = \sqrt{p}\left[-\Delta_r \cos L + [(w+1)\sin L + g]\,\frac{\Delta_t}{w} + (h\sin L - k\cos L)\frac{g\Delta_n}{w}\right] \\ \dot{h} &= \frac{dh}{dt} = \sqrt{p}\frac{s^2\Delta_n}{2w}\cos L \\ \dot{k} &= \frac{dk}{dt} = \sqrt{p}\frac{s^2\Delta_n}{2w}\sin L \\ \dot{L} &= \frac{dL}{dt} = \sqrt{p}\left(\frac{w}{p}\right)^2 + \frac{1}{w}\sqrt{p}(h\sin L - k\cos L)\Delta_n \end{cases} \tag{10}$$

By setting $\mu = 1$ and scaling the other quantities accordingly, the problem results better bounded as p, for these type of orbits, is always around 1 AU and all the other quantities except for the longitude L are already bounded between -1 and 1.

A validation of this set of scaled equations was conducted before they were implemented into DMG. Starting from a very simple initial state $[p, g, f, h, k, L, m]$of:

$$\text{initial state} = [1, 0, 0, 0, 0, 0, 1]$$

For the scaled elements and of

$$\text{initial state} = [l_c, 0, 0, 0, 0, 0, m_{init}]$$

For the unscaled one, they were propagated using the Matlab function ode45 for a period of 200 days, with a constant thrust of 0.135 N in the tangential direction. The results, as can be seen in the plots below, are identical, both reaching a final mass of 1420 kg and the same spatial position and velocity.

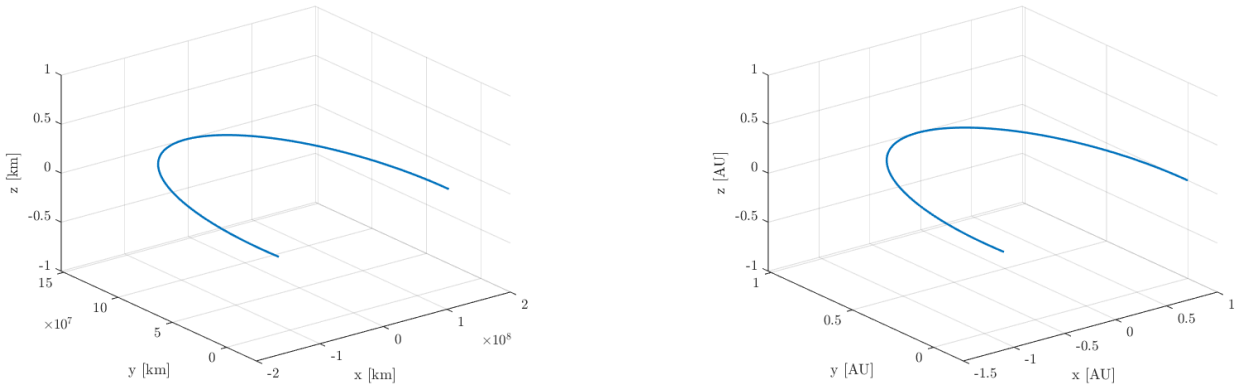

(a) Propagation for the unscaled elements.

(b) Propagation for the scaled elements.

Figure 7: Scaling of MEE.

Contrary to theoretical expectations, Modified Equinoctial Elements (MEEs) performed worse than Cartesian State Vectors (CSVs) in multi-phase optimization problems. This was surprising since MEEs offer several apparent advantages: four of the six elements are naturally bounded between -1 and 1, all GTOC-4 asteroids have semi-parameters under 1.3 AU, and these elements remain constant in unperturbed orbits. In low-thrust scenarios, where perturbations are small, MEEs should change gradually, theoretically providing better numerical stability than CSVs, which experience significant variations in position and velocity throughout each orbit. Several hypothesis were made to explain this behaviour:

- **Non-linear relationships**: The transformation between MEEs and physical spacecraft position/velocity is highly non-linear. In the setup, the event constraints are computed using these relations, which might complicate finding a state which respect such constraint reliably.
- **Initial guess conversion**: The Sims-Flanagan initial guesses was originally generated in Cartesian coordinates. Converting these to MEEs might have introduced small errors that might affect convergence.

For the orbits considered, which have a very low inclination and eccentricity, f, g, h and k are very close to 0. That might explain the numerical challenges encountered so far. A scaling procedure to bring such elements closer to 1 was implemented but it didn't improve the performances.

Furthermore, it has been tried to use directly a set of equinoctial elements as the event constraint, bypassing the conversion to cartesian. This is not feasible in the context of the optimization for the flybys as imposing a set of elements would also constraint the velocity of the spacecraft. This trial was also unsuccessful in improving the performances.

6.2 Initial Guesses

Initial guesses played a critical role in the optimization process, with several approaches explored. Of the 4 methods presented in subsection 5.1, only the Sims-Flanagan was utilized during the third semester, as it proved to be the most effective by providing near-feasible initial trajectories. This model discretized the trajectory into segments, modeling low-thrust actions as impulsive ΔVs followed by Keplerian propagation, creating high-quality first approximations that significantly improved convergence. These initial guesses were used to get completely feasible trajectories without optimizing for any variable. Such solutions were then implemented themselves as an initial guess when using an objective function.

6.3 Optimization strategies

When approaching complete trajectory optimization, two primary methodologies were compared: full-trajectory simultaneous optimization and sequential arc-by-arc optimization. The full-trajectory approach attempted to optimize all mission phases at once, maximizing the freedom given to the solver to operate on the whole trajectory, but requiring substantial computational resources. The sequential approach optimized goes through the whole trajectory incrementally, starting from the first arc and proceeding forward by one arc at each successive optimization. This gives the solver the possibility to gradually adjust the states of the previous segments to a feasible one for the last arc of the batch.

Through systematic testing, it was determined that optimizing six trajectory arcs simultaneously while progressively shifting forward provided the optimal balance between computational efficiency and solution quality. This sequential methodology allowed sufficient flexibility for the solver to account for interactions between adjacent trajectory segments while keeping computational demands manageable.

6.4 Objective functions

Expanding on what was presented in subsection 5.1, the use of a Lagrange cost functional was briefly considered to speed up convergence for feasible arcs and to try to better guide the solver towards a feasible solution for problematic arcs. This additional cost function is a vector of length equal to the number of nodes in the trajectory, whose components must be minimized. A Lagrange cost function of the following type was implemented:

$$Lagrange = k \cdot T \tag{11}$$

Where T is the magnitude of the thrust at every node of the trajectory, and k is a scalar weight to give to the Lagrange part of the cost function more or less importance. Values of k between 0.01 and 0.1 were considered.

This cost formulation had the scope to more aggressively guide the solver towards a minimum thrust, and thus maximum mass solution. This formulation yielded no real improvement in arcs feasibility and slowed down convergence while not improving the final mass of the spacecraft and was not therefore pursued.

Another formulation using just the Lagrange constraints, thus setting Mayer = 0 (which should yield the same solution as minimizing the thrust at each control point is the same as maximizing the final mass) was tried, but, as expected it performed worse as the solver needed to account for multiple optimization varialbes along the trajecotey instead of just one.

7 Results and Analysis - Johnson solution

In this section, another solution for the GTOC-4 challenge was analyzed. This solution was presented by *Gregory Phillip Johnson* in [4] after the end of the challenge to benchmark his algorithm for spacecraft tours. His best solution is composed of 45 arcs (thus visiting 46 asteroids), with a final mass of 506.24 kg, as can be seen in Table 2.

no.	t (MJD)	mass (kg)	Asteroid	no.	t (MJD)	mass (kg)	Asteroid
0	58629.41	1500.00	Earth	1	58713.42	1500.00	2006QV89
2	58815.69	1470.01	2003YT70	3	58922.79	1449.25	2008CL20
4	59003.68	1405.84	2005ED318	5	59062.81	1392.57	2005NW44
6	59162.22	1367.57	2007TK15	7	59199.40	1351.71	2005GA120
8	59265.91	1343.26	2006KQ1	9	59406.16	1300.46	2001GO2
10	59523.95	1273.81	2000RN77	11	59604.68	1237.90	2003SW130
12	59674.94	1221.59	162173	13	59792.74	1183.36	2007DS84
14	59891.76	1139.15	2005BC	15	59969.68	1116.96	2008SW7
16	60025.00	1094.31	2003WY153	17	60113.15	1075.84	1998DK36
18	60186.68	1058.79	2002JR100	19	60256.89	1032.36	2008NQ3
20	60326.59	1007.38	2006RJ7	21	60396.51	988.81	2007US12
22	60481.29	961.61	2004YC	23	60532.90	947.45	2005CN
24	60635.94	922.78	2007LF	25	60790.26	910.34	2004TP1
26	60853.27	902.49	2005XY4	27	60912.49	881.65	162157
28	60986.19	860.20	2005GY8	29	61071.24	831.07	68372
30	61162.56	806.94	2008TC3	31	61236.31	794.12	2004JN1
32	61298.81	771.87	175729	33	61368.96	750.65	2007YF
34	61449.31	739.09	2006UB17	35	61512.08	718.63	2005NE21
36	61557.33	698.63	2004RU109	37	61634.61	685.94	2000UG11
38	61734.14	664.80	2004PR92	39	61800.31	645.00	162416
40	61874.01	630.55	2006WQ29	41	61933.24	607.81	2007RE2
42	61959.06	601.32	2001SE270	43	62032.77	588.42	2002XV90
44	62103.03	574.49	2007DS7	45	62202.56	545.42	2004CZ1
46	62273.00	506.24	2006BZ147				

Table 2: Johnson's solution. Taken directly from [4]

The work carried out used Yago Castilla's first guesses with the Sims-Flanagan method as an essential component for the optimization.

The guess obtained by the Sims-Flanagan method, while close to being feasible, presents a maximum thrust higher than the allowed 0.135N in the arcs present in Table 3

Arc Number	5	6	7	8	9	10	11	12	29	30	31
Max Thrust [N]	0.1391	0.1396	0.1404	0.1364	0.1364	0.1451	0.1432	0.1417	0.1477	0.1470	0.1461

Table 3: Thrust violations in the Sims-Flanagan Johnson solution guess.

Furthermore, the mass of the guess is not continuous, as at every new arc the mass was set to be the one of the original Johnson solution and continuity between the final mass of one arc and the initial mass of the next arc was not imposed. The mass and thrust histories of the initial guess can be seen in Figure 8.

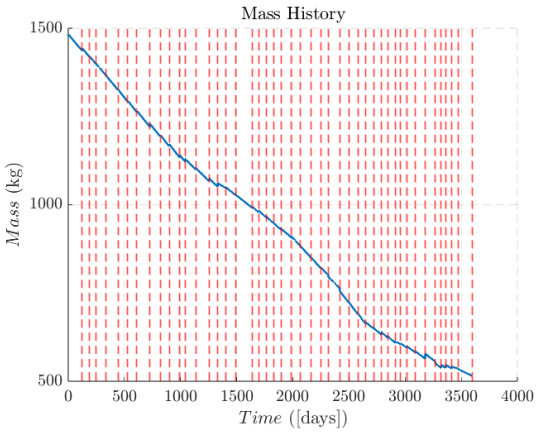

(a) Mass History.

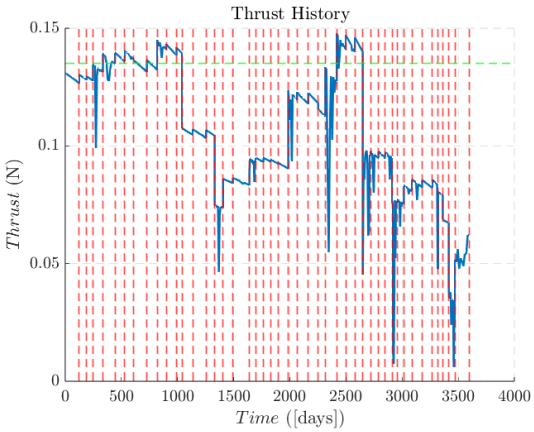

(b) Thrust History.

Figure 8: Sims-Flanagan guess for the Johnson solution.

Little jumps in the mass, especially towards the last segments, can be observed. Regarding the thrust, for the majority of the arcs a thrust under 0.135 N (the green line in Figure 8 (b)). Generally speaking, in every arc the thrust results to be higher at the beginning of the arc, gradually decreasing as the spacecraft approaches the target asteroid. The average thrust for the whole solution is 0.1048 N.

7.1 Full solution without optimization

To assess the problem's feasibility, a Cartesian State Vector approach was initially used to evaluate whether the entire solution could satisfy the GTOC-4 challenge's thrust and mass constraints. As discussed in subsection 5.1, the approach was to set Mayer = 0 as the objective function, focusing solely on finding a viable solution without truly optimizing for anything.

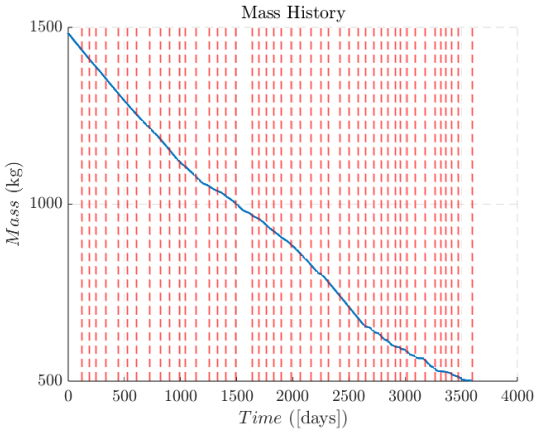

(a) Mass History.

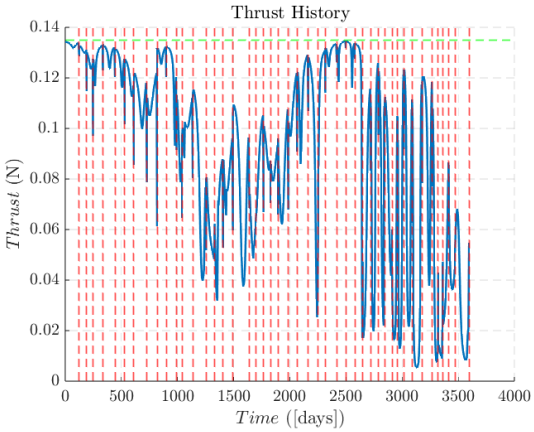

(b) Thrust History.

Figure 9: Non-optimized feasible solution for the Johnson trajectory.

The DMG solver found a solution that just barely met the minimum mass requirement of 500 kg (with a final mass of 500.55 kg) while maintaining thrust values below the 0.135 N limit in all trajectory arcs, with an average thrust of 0.0896 N. When comparing Figure 9(b) with Figure 8(b), it is noticed that the DMG solution applies more aggressive thrust in already-feasible arcs. This likely occurs because reducing thrust to acceptable levels in problematic arcs required compensatory higher thrust during preceding segments.

This procedure proved that the Johnson solution is feasible with the GTOC-4 constraints. Now, it is a matter of finding an optimized solution in terms of the final mass.

7.2 Attempt at full solution maximizing the mass

The next step was to try to optimize the whole solution at once, this time maximizing the final mass at the end of each phase. The non-optimized feasible solution previously obtained was used as the initial guess for this run. This is because having an already feasible solution as an initial guess might ease the convergence.

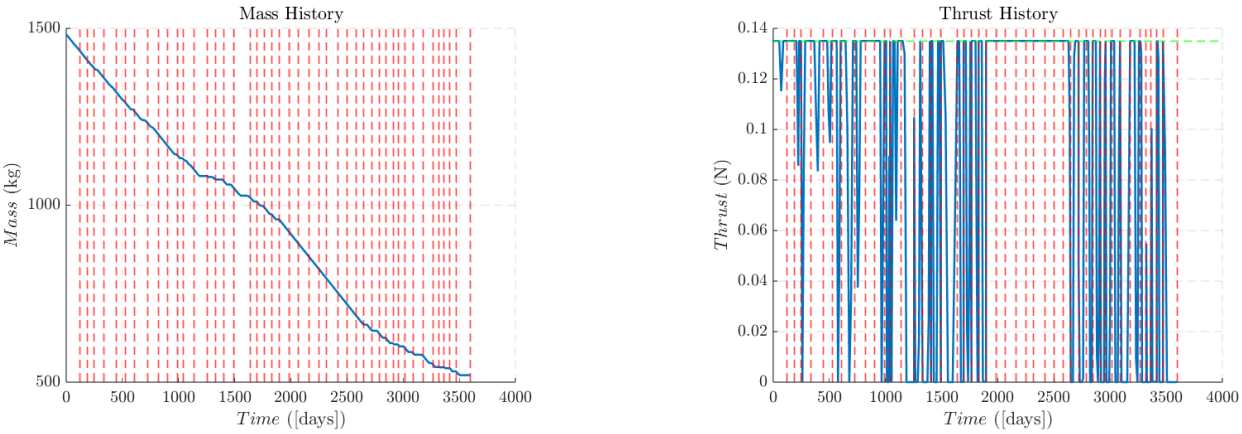

(a) Mass History.

(b) Thrust History.

Figure 10: Full solution for the Johnson trajectory - Restoration failed.

The run was not entirely successful, as a *Restoration failed error* occurred. Nonetheless, the output solution had a final mass of 519.6 kg, with a much more aggressive thrust switching, albeit with a lower average thrust of 0.0890 N, as expected as the final mass is slightly higher.

Optimizing the full solution at once presents significant computational challenges. While this approach would allow GPOPS to determine the optimal combination of state and control variables across the entire trajectory, maximizing final mass while respecting all constraints, it proves to be prohibitively expensive from a computational standpoint. Processing all 45 phases simultaneously requires handling thousands of variables, creating excessive memory demands and computation times that make this approach impractical (in the order of days) for standard computing resources. It was attempted to implement the problem on ISAE-SUPAERO's high performance computing system RAINMAN to address the computational demands. However, as of the time of writing this report, installation issues with DMG on this system prevented the successful implementation of this approach.

7.3 Sequential optimization

Building on the non-optimized solution presented in 7.1, a sequential approach to optimize the Johnson trajectory was implemented. Starting with the feasible baseline solution as the initial guess, a limited number of trajectory arcs were optimized at a time to maximize final spacecraft mass.

After each optimization round, the starting arc was shifted forward by one segment, allowing to progressively refine the entire trajectory. This sequential method enabled to focus computational resources on smaller portions of the trajectory while ensuring continuity and constraint satisfaction across the complete solution.

When attempting to optimize the trajectory sequentially, an important balance must be maintained. Optimizing too few arcs at once prevents the solver from finding feasible solutions when shifting forward. This occurs because each arc's initial state depends significantly on maneuvers performed in previous segments. The solver requires sufficient flexibility to determine viable initial conditions for reaching subsequent asteroids. These conditions result from maneuvers performed across multiple consecutive legs.

7.3.1 Batch of 4 arcs

The first trial involved optimizing the solution 4 arcs at a time. This has proven not to be entirely successful as many of the optimization runs ended with a *restoration failed* exit, meaning that the solver was unable to find a true optimal solution. The average thrust of this solution was of 0.0894 N, with a final mass of 524.4 kg.

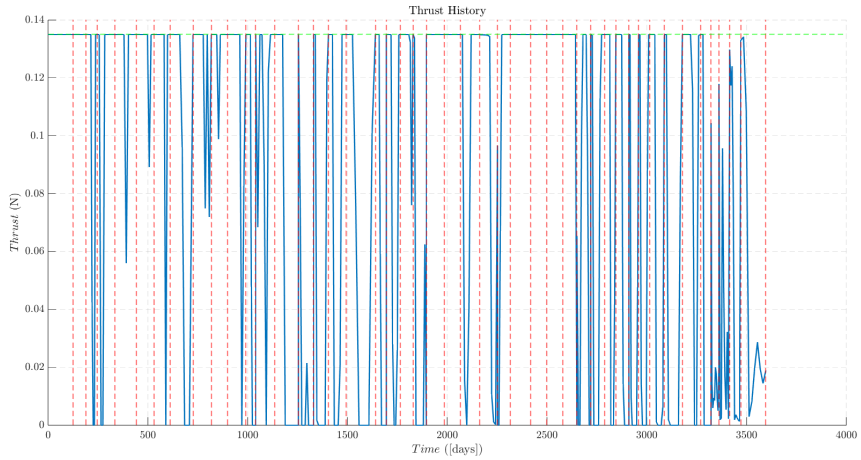

Figure 11: Thrust history, optimizing 4 arcs at a time.

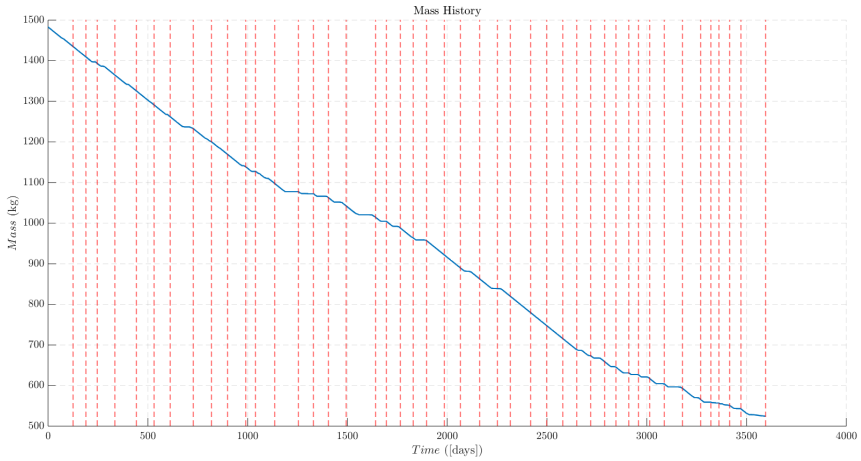

Figure 12: Mass history, optimizing 4 arcs at a time.

This can be clearly seen towards the last arc of the solution, where the thrust profile is erratic, with the thrust exhibiting many sudden changes. Looking more closely at the thrust history graph, we can observe a pattern of instability that becomes particularly pronounced in the final segments. These abrupt changes in thrust direction and magnitude indicate that the solver is struggling to find consistent control inputs that satisfy the boundary conditions. The "restoration failed" exits mentioned in the context suggest that when optimizing only 4 arcs at a time, the algorithm lacks sufficient freedom to resolve these inconsistencies. The solver appears to be compensating for suboptimal decisions in previous segments by making increasingly extreme corrections in later arcs. Without enough overlapping arcs in the optimization window, the solver cannot properly account for how early maneuvers affect future flybys, leading to the forced, unnatural control behavior visible in the graph. A larger optimization window would likely produce smoother thrust profiles by allowing the solver to better distribute maneuvers across longer arcs of the trajectory.

7.3.2 Batch of 6 arcs

Through trial and error, it was determined that optimizing 6 arcs simultaneously provides the ideal balance between computational efficiency and solution quality, giving the solver enough maneuvering room while keeping computational demands manageable.

With the same setup as the previous optimization, but optimizing a batch of 6 arcs at once, the following solution was produced. This time, every optimization sequence was terminated either with "*optimal solution*

found" or "*solved to acceptable level*", which, while meaning that this is not truly the optimal solution, it is within the tolerances that the solver consider acceptable.

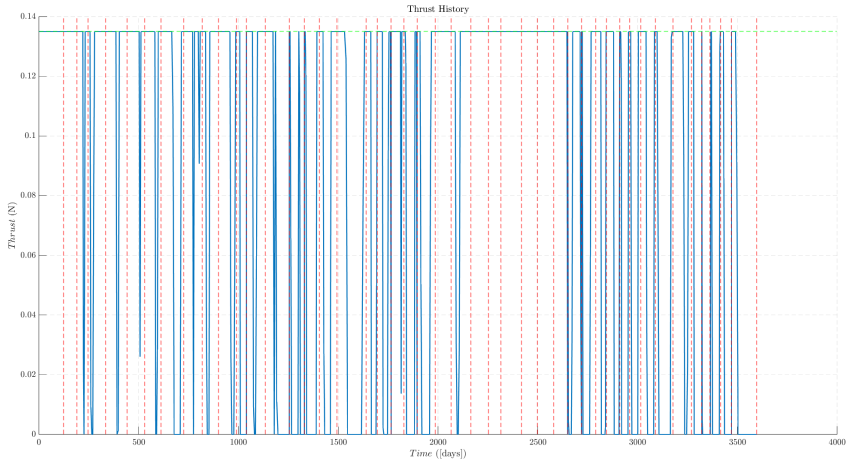

Figure 13: Thrust history, optimizing 6 arcs at a time.

The thrust profile shown in Figure 13 exhibits more consistent patterns compared to the 4-arc case, lacking the erratic behavior observed toward the end of the previous solution. By providing the solver with sufficient flexibility to distribute maneuvers across longer trajectory segments, it was able to develop smoother and more efficient control strategies. The optimal engine on-off switching behavior is clearly visible, with well-defined thrust periods separated by coast arcs.

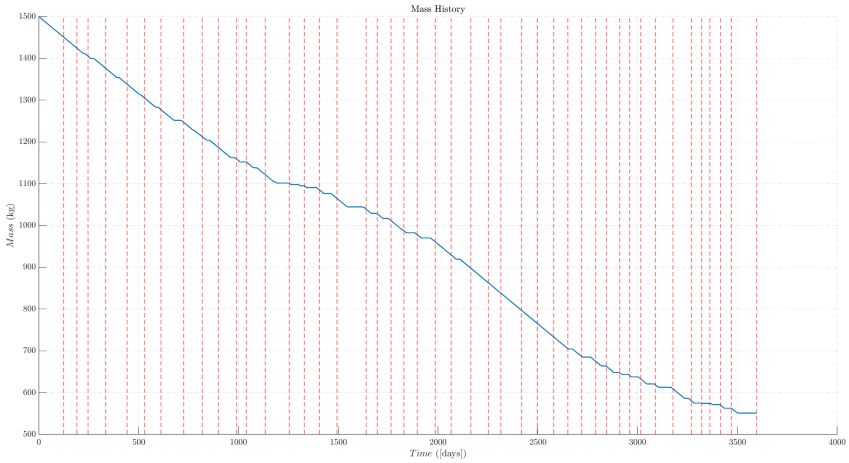

Figure 14: Mass history, optimizing 4 arcs at a time.

Examining the mass history in Figure 14, a relatively steady propellant consumption rate throughout the mission can be observed, with slightly lower consumption rates in certain mission phases. This indicates that the solver successfully identified optimal trajectories that minimized propellant usage while satisfying all rendezvous constraints.

The final mass of this solution is 550.95 kg, with an average thrust of 0.0880 N, the lowest among the solutions obtained in this study. This represents a significant improvement over both the non-optimized solution (500.55 kg) and the partially optimized 4-arc approach (524.4 kg), demonstrating the effectiveness of this optimization strategy.

7.4 Comparison

One of the most important features of the sequential optimization is the ability to successively refine the same arc across multiple runs. For instance, running a 6 arcs batch optimization allows to optimize 6 times the arcs from 6 to the end, each time adapting to meet the constraints of the flyby for the new asteroid in the sequence.

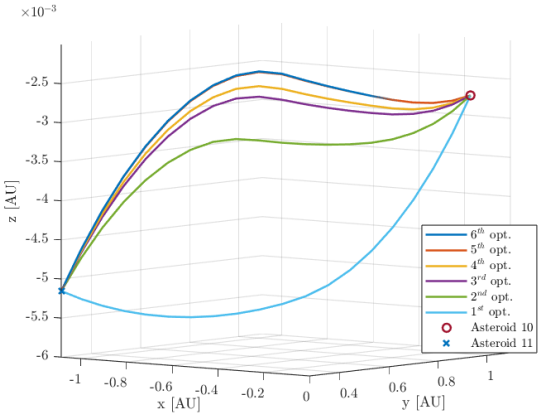

(a) Trajectory evolution during optimization.

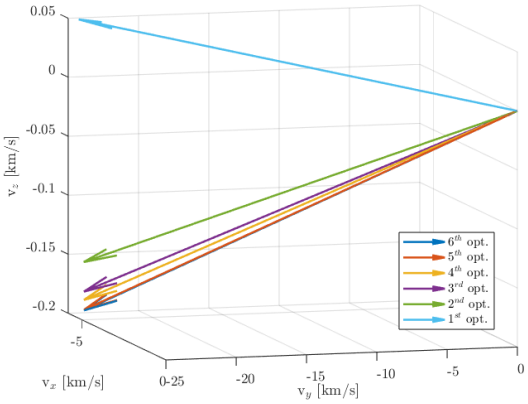

(b) Final velocity evolution during optimization.

Figure 15: Comparison of different optimization stages, arc 10.

Figure 15 illustrates this process for arc 10, showing how both the spatial trajectory and velocity profiles evolve across optimization iterations. Each colored line represents the same arc optimized in different contexts, from being the last arc in the window (1^{st} optimization) to being the first arc (6^{th} optimization). In Table 4 the evolution of the final mass of the arc is presented. It can be noted that the mass decreases at every iteration but the last. This is due to the fact that, in order to render feasible the following arcs, more thrusting is required in the previous ones. Furthermore, at each iteration the solution changes less and less, meaning that the more distant arcs taken into account have less and less influence. The 5^{th} and 6^{th} iterations are basically identical, meaning that the addition of a 6^{th} asteroid does not have a significant influence on the trajectory. Adding more asteroids would therefore increase the computational complexity without significantly improving the result.

Mass evolution	
Run	Mass [kg]
1	1211
2	1192
3	1189
4	1188
5	1186
6	1186

Table 4: Mass evolution through the optimization.

The main takeaways of using this method are:

- **Contextual Optimization:** Each iteration incorporates more information about future mission requirements, leading to solutions that balance immediate constraints with long-term efficiency.
- **Trajectory Evolution:** While all versions successfully reach the target asteroid, their approach trajectories differ based on the optimization context.
- **Global Performance:** The final optimized trajectory (6^{th} iteration) benefits from knowledge of five subsequent arcs, resulting in a solution that approaches global optimality while remaining computationally feasible.

8 Results and Analysis - Moscow original solution

The same optimization strategies mentioned in section 7 were used to study the feasibility of the Moscow original solution composed of 43 asteroids. Starting from the full non-optimized solution with a maximum thrust of 0.2 N, it was first tried to slowly lower the maximum thrust allowed by the optimizer hoping to steer the solver towards a feasible solution respecting the thrust constraint of 0.135 N. This did not work as the solver would always converge to an unfeasible solution when lowering the maximum thrust.

A new, almost feasible initial guess provided by Yago Castilla with his work on the Sims-Flanagan method was also used. As can be seen in Figure 16, the thrust is higher than the maximum allowed only for very short segments and it is still very close to the maximum thrust of 0.135 N. This guess optimized the dates of the flybys to find more favourable asteroids position, lowering the amount of thrust required to reach them.

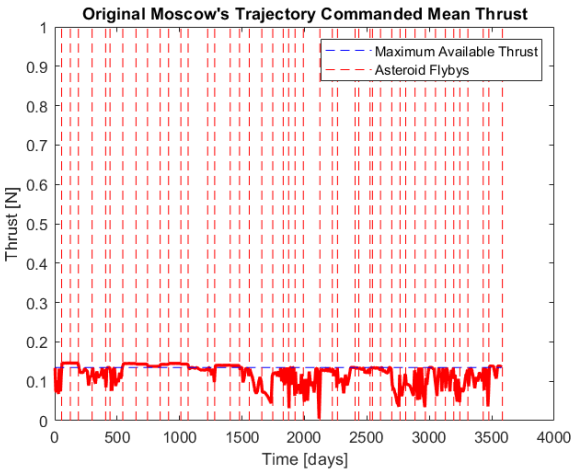

Figure 16: Sims-Flanagan's almost feasible guess. Courtesy of Yago Castilla.

Even with this quasi-feasible guess, GPOPS would not converge to a feasible solution, especially for the first arcs. This is surprising because GPOPS managed to find a solution for the Johnson trajectory, whose initial guess violated the thrust constraints too. A possible explanation could be that the first maximum thrust violation in the Johnson guess started on the 5^{th} arc, giving the optimizer enough room to adjust the previous leg to make the problematic one feasible. In the Moscow guess, the maximum thrust is above the threshold already in the second arc, not leaving GPOPS enough manouvering room on the previous legs to make such arc converge.

9 Conclusion

This study investigated the application of DMG, a modified version of the GPOPS-II optimizer, to complex low-thrust trajectory problems within the GTOC-4 challenge framework. Through systematic analysis of different optimization approaches, state representations, and initial guesses, significant insights were gained into the feasibility and optimization of multi-asteroid rendezvous missions. The initial focus on the Moscow solution revealed significant computational challenges for complex multi-phase trajectories. While technically feasible with increased thrust limits, achieving convergence with the competition's 0.135 N constraint proved difficult. This led to exploration of the Johnson solution, which yielded more promising results.

The implementation of a scaling procedure for the Modified Equinoctial Elements representation was considered to improve numerical stability, but a Cartesian State Vector representation generally demonstrated better convergence characteristics in multiple-phase problems. The study confirmed the critical importance of high-quality initial guesses, with the Sims-Flanagan model providing valuable first approximations that significantly improved convergence.

One of the most significant findings was the effectiveness of sequential optimization compared to whole-trajectory optimization. By optimizing 6 trajectory arcs simultaneously and progressively shifting forward, an optimal balance was achieved between computational efficiency and solution quality. This approach successfully verified the feasibility of the Johnson solution under GTOC-4 constraints, achieving a final spacecraft mass of 550.95 kg, well above the minimum requirement of 500 kg.

The failed optimization of the Moscow solution shows how low-thrust optimization problems, especially the ones as complex as multi-asteroid tours, are difficult to optimize and how small variations in the initial conditions or in the optimization landscape can severely impact convergence, as such problems often lay on the boundary between feasibility and infeasibility.

References

[1] European Space Agency. Gtoc4 problem description. Technical report, European Space Agency, 2010. Global Trajectory Optimization Competition.

[2] David Morante González. *User's Manual for DMG Version 1.0: A MATLAB® Software for Solving Multiple-Phase Optimal Control Problems based on GPOPS*. Avenida de la Universidad 30, Leganés, Madrid 28911, 2021. Derived work from the open-source project GPOPS 2.2.

[3] I. S. Grigoriev and M. P. Zapletin. Choosing promising sequences of asteroids. *Automation and Remote Control*, 74(8):1284–1296, 2013. Original Russian Text published in Avtomatika i Telemekhanika, 2013, No. 8, pp. 65-79.

[4] Gregory Phillip Johnson. *A Tabu Search Methodology for Spacecraft Tour Trajectory Optimization*. Dissertation, The University of Texas at Austin, December 2014.

[5] David Morante, Manuel Sanjurjo Rivo, and Manuel Soler. A survey on low-thrust trajectory optimization approaches. *Aerospace*, 8(3):88, 2021. Academic Editor: Roberto Sabatini.

[6] Jon A. Sims and Steve N. Flanagan. Preliminary design of low-thrust interplanetary missions. In *AAS/AIAA Astrodynamics Specialist Conference*, pages AAS 99–338, Girdwood, Alaska, August 1999.

[7] M. J. H. Walker, B. Ireland, and J. Owens. A set of modified equinoctial orbital elements. *Celestial Mechanics*, 36:409–419, 1985.